Crystallization and differentiation of Archean komatiite lavas from northeast Ontario: phase equilibrium and kinetic studies

ROSAMOND J. KINZLER AND TIMOTHY L. GROVE

Department of Earth, Atmospheric and Planetary Sciences
Massachusetts Institute of Technology
Cambridge, Massachusetts 02139

Abstract

Phase equilibrium experiments on two synthetic komatiite compositions have been used to develop a liquidus diagram that allows prediction of phase appearance sequences and crystallization paths for Munro Township komatiite lava flows. The experimentally determined phase relations and the observed mineral associations in thick, layered komatiite flows (e.g, Fred's Flow and the Alexo Flow) provide information on the bulk composition of these Munro komatiite lavas, the liquid line of descent and the magmatic processes that accompanied cooling and differentiation. Under equilibrium conditions a lava with bulk composition similar to that of Fred's Flow or the Alexo Flow should crystallize olivine as the liquidus phase, followed by spinel, pigeonite, plagioclase and finally augite. Komatiite lavas which have crystallized pigeonite as the first pyroxene are restricted to a limited range of bulk magma compositions. Cooling rate experiments reproduce successfully the mineral assemblages, the pyroxene zoning trends and the general textural characteristics of the olivine and pyroxene spinifex zones. In the upper part of the lava flow fractional crystallization of olivine moved the residual liquid composition into the pigeonite primary phase volume. Pigeonite crystallized, the liquid line of descent departed from equilibrium and augite and plagioclase crystallized under supercooled conditions. In the interior of these flows, within-flow magma mixing may have been important during the later stages of solidification, if the flow solidified under closed-system conditions.

Introduction

Komatiitic lavas from the Munro Township, northern Ontario display unusual bulk chemical variations and mineralogical associations that have been difficult to reconcile through any simple origin by fractional crystallization during cooling and differentiation. Two Archean lava flows of northern Ontario, Fred's Flow and the Alexo Flow have been studied extensively by Arndt and coworkers, and are the subject of this experimental study. The most unusual characteristics of these layered flows are the pyroxene associations. Augite is found in the olivine spinifex layer, pigeonite and augite in the pyroxene-spinifex layer and orthopyroxene and augite assemblages are found in the interior gabbroic portion and lower cumulus layers. The purpose of this experimental study is to determine the 1-atmosphere phase relations for these komatiites and to use this information to infer the magmatic processes that have combined to produce the observed mineral associations. In the following discussion we describe the phase relations determined using synthetic analogs of komatiite lavas, then we predict the crystallization sequence that would be expected

during cooling and crystallization of the komatiite lava parental to Fred's Flow and the Alexo Flow. Next, we show how kinetic factors influence the phase appearance sequence and mineralogy and finally we present a model for the crystallization and differentiation of Fred's flow.

Both of these komatiitic lava flows developed layering during differentiation and cooling. In Fred's Flow the layering has been divided into four zones by Arndt et al. (1977): a brecciated or spinifex upper unit, a gabbroic interior, a lower cumulate zone and a basal zone (Fig. 1). The upper chilled margin consists of a brecciated olivine porphyry, which overlies spinifex-textured rock that contains skeletal olivine phenocrysts in a glass + augite groundmass. Below this olivine-spinifex zone is a thicker pyroxene-spinifex layer. The pyroxene phenocrysts are internally skeletal with pigeonite cores and augite rims and are enclosed in a groundmass of augite and plagioclase. The second zone is gabbroic and contains plagioclase, augite and bronzitic orthopyroxene. This gabbroic unit lies on a cumulate of augite and bronzite which is underlain by a thick olivine cumulate zone. The basal border zone of the flow consists of medium-grained olivine in a groundmass of augite, plagioclase and altered
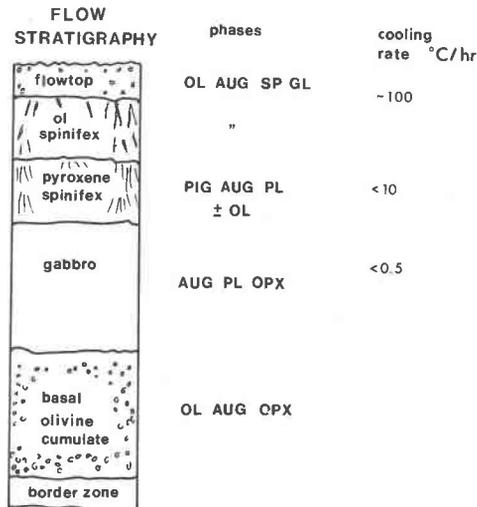
Fig. 1. Cross section of Munro Township spinifex layered komatiite flows showing the stratigraphic zones described in Arndt et al. (1977). Cooling rates for the upper portions of the flow are inferred from the pyroxene compositions produced in dynamic crystallization experiments. Abbreviations for the phases are found in footnote to Table 1.

orthopyroxene. Detailed descriptions of these lava flows may be found in Arndt et al. (1977), Arndt (1977) and Arndt and Fleet (1979).

Sample selection

One important problem that must be solved before any experimental study of Archean komatiites can be undertaken is to determine the bulk composition of the lava flow. We used two bulk compositions for our investigation. The first (composition A, Table 3) was an estimated bulk composition of Fred's Flow made by averaging the analyses of the A1 zone of two drill sections through a peridotitic komatiite flow (Arndt et al., 1977, Table 6). The A1 zones of these flows had well-developed spinifex textures. From this bulk composition estimate, olivine was removed by a fractional crystallization calculation until a Fo_{85} olivine was on the liquidus, and this evolved liquid was used as the starting composition. The second starting composition (composition B, Table 3) was made by averaging seven analyses of the B2 zone of two drill sections through the same flows described above. The B2 zones are olivine cumulates which consist of equant olivine in a matrix of pyroxene and devitrified glass. From this average composition, olivine was removed by calculation until the composition was in equilibrium with Fo_{90} olivine.

The major uncertainties in estimating the bulk compositions of large differentiated lava flows, like Fred's Flow, are three: (1) the chilled margins, which should represent a liquid composition are rubbly, brecciated and weathered, and are highly suspect, (2) the flow interior is highly differentiated and it is possible that the interior zones are cumulates or crystalline residues of fractionation that are not representative of liquid compositions, and (3) alteration by seawater and metamorphism may have changed the rocks' compositions. These factors have probably

affected the compositional integrity of most of the layers in these ancient komatiite flows, and one of the results of this study will be to suggest compositional limits on the parent magma for Fred's Flow and the Alexo Flow. We will also suggest some guidelines for estimating the bulk compositions of differentiated ultramafic lava flows based on the mineralogy of the differentiated layers.

Experimental petrology

Experimental and analytical methods

The compositions chosen for the experimental investigation were prepared as oxide mixes using Johnson-Matthey high purity SiO_2, MgO, Al_2O_3, TiO_2 Cr_2O_3 and MnO. The alkalies were weighed in as $NaSiO_3$ and $K_2Si_4O_9$ and CaO was added as $CaSiO_3$. Iron was added as FeO using Fe sponge and Fe_2O_3. Each oxide mix was ground in an agate mortar for 6 hours, the Fe sponge was added and the mix was ground an additional 1.5 hours. The resulting homogeneous oxide mixes were pressed into discs using an XRF pellet press with elvanol as a binder. Small chips (25 to 45 mg) were broken from the oxide discs and used for the experiments. The chips were sintered with an oxygen–natural-gas torch to 0.004″ diameter FePt alloy loops that were fabricated following the method of Grove (1981) to contain 9 to 10 wt.% Fe. This alloy minimized iron exchange between the silicate charge and the loop. The loop and sample were suspended in the hotspots of Deltech DT31VT quenching furnaces in atmospheres of CO_2–H_2 gas. Temperature was monitored using Pt-Rh10 thermocouples calibrated against the melting points of gold and palladium on the IPTS 1968 temperature scale. Oxygen fugacity was monitored using ZrO_2–CaO electrolyte cells calibrated at the Fe–FeO and Ni–NiO buffers. The results of synthesis experiments performed near the quartz–fayalite–magnetite (QFM) buffer are presented in Tables 1 and 3. Cooling rate experiments (Table 2) were performed by melting the starting mix at an initial temperature specified in Table 2. The run was then cooled at a linear rate and terminated at a desired temperature by quenching into water. Cooling rate control was achieved using Eurotherm 125 temperature programmers wired into the control thermocouple circuit of the furnaces. The programmer added a linear signal at a desired rate to control temperature drop.

Compositions of phases were obtained with the MIT 3-spectrometer MAC-5 electron microprobe using on-line data reduction and matrix correction procedures of Bence and Albee (1968) with modifications of Albee and Ray (1970).

Phase relations and liquid line of descent

Olivine is the liquidus phase in composition B (Fig. 2) at ~1366°C. Spinel joins olivine at 1320°C, and pigeonite appears in the crystallization sequence at 1205°C, after about 20% solidification. By 1185°C plagioclase has appeared as a crystallizing phase. The liquidus was not determined for composition A, but olivine and spinel are both present at 1250°C, the highest temperature experiment performed on this composition. The first pyroxene to form is augite at ~1195°C, and plagioclase has joined the crystallization assemblage at 1180°C.

The compositions of liquids produced in the 1-atmosphere experiments were recalculated from wt.% oxides

Table 1. Run conditions and run products for synthetic komatiitic compositions.

Run #	T (°C)	Duration (hrs.)	Run[*] Products	log fO$_2$
Composition A				
3	1173	95.7	gl-pl-aug-ol-sp	-8.78
5	1187	47.9	gl-aug-ol-sp	-8.74
1	1202	23.8	gl-ol-sp	-8.46
2	1223	46.8	gl-ol-sp	-8.19
4	1247	47.7	gl-ol-sp	-7.81
Composition B				
4	1173	136.2	gl-pl-pig-ol-sp	-8.94
2	1176	71.9	gl-pl-pig-ol-sp	-8.68
3	1184	93.7	gl-pig-ol-sp	-8.58
1	1196	45.2	gl-pig-ol-sp	-8.41
5	1206	21.3	gl-ol-sp	-8.14
6	1225	25.1	gl-ol-sp	-8.03
7	1244	21.8	gl-ol-sp	-7.79
17	1255	23.9	gl-ol-sp	-8.02
12	1270	18.2	gl-ol-sp	-7.80
16	1294	25.2	gl-ol-sp	-7.54
25	1304	31.9	gl-ol-sp	-7.38
24	1321	22.8	gl-ol-sp	-7.12
31	1347	24.2	gl-ol	-6.82
35	1359	10.1	gl-ol	-6.72
34	1371	16.0	gl	-6.56

[*] Abbreviations: gl=quenched liquid, ol=olivine, sp=spinel, pig=pigeonite, aug=augite, pl=plagioclase.

into oxygen-normalized mole units of the components olivine (ol), clinopyroxene (cpx), plagioclase (plag), orthoclase, silica (qtz) and spinel. This six-component system was simplified by projecting into the tetrahedron ol–cpx–plag–qtz and further simplified by projection through plag into the ol–cpx–qtz pseudoternary (Fig. 3.). This ternary subprojection will be used to discuss the compositional variation followed during differentiation of komatiite flows. The discussion must be approximate, because it is impossible to be completely rigorous when one has simplified ten-component space into 3 or 4 components by projection. One limitation of the ol–cpx–qtz subprojection is that most of the liquids displayed on the projection are not plagioclase-saturated, so the subprojection is not strictly valid. We feel that the projection provides a useful visual representation of the liquid-line-of-descent, and therefore we retain it. The residual liquids from the experiments performed on the two komatiite bulk compositions locate portions of the ol–cpx–plag cotectic and the ol–pig–plag reaction curve. The komatiite system boundary curves are close, but shifted slightly toward the olivine corner of the projection when compared to the 1-atmosphere plagioclase-saturated cotectics and reaction curves located by Walker et al. (1979) and Grove et al. (1982) for tholeiitic and calc-alkaline systems. Since the komatiites are much lower in TiO$_2$, Na$_2$O and K$_2$O, such differences in the projected positions of saturation surfaces are not surprising. We have sketched in a topology for the 1-atmosphere komatiite

diagram which is similar to that found in Fo–Di–Qtz by Kushiro (1972) and by Grove et al. (1983) for the tholeiitic and calc-alkaline natural system. A difference from the topology of Grove et al. (1983) is that a thermal divide is absent on the ol–pig±plag reaction curve (see Grove et al. (1983) for a discussion).

Discussion

Predicted crystallization sequence for komatiite flows

For composition B crystallization begins with olivine as the liquidus phase followed by spinel. As shown in Figure 3 crystallization of olivine and spinel moves the liquid away from the projection of the bulk composition of B toward the olivine–pigeonite reaction curve. When the liquid reaches the curve, olivine and liquid react to form pigeonite, and under equilibrium conditions the liquid follows the reaction boundary toward the piercing point where plagioclase and augite join the crystallization assemblage. The projected position of the liquid will remain at this piercing point, until solidification is complete, olivine + liquid reacting to form pigeonite, augite and plagioclase. For composition A, the later phase appearance sequence differs in the order of pyroxene crystallization. After crystallization of olivine and spinel the liquid

Table 2. Results of cooling rate experiments on synthetic komatiitic composition B.

Run #	T °C	duration (hrs.)	T fin	duration (hrs.)	Rate °C/hour	Run[*] Products
42	1292	3.6	975	672.6	0.47	ol-sp-pig-aug rim-pl-gl
18	1292	6.4	1112	281.5	0.57	ol-sp-pig-aug rim-pl-gl
32	1290	2.3	1166	304.7	0.41	ol-sp-pig-aug rim-gl
26	1273	4.6	1200	161.8	0.45	ol-sp-pig-ql
11	1267	6.4	980	297.1	0.97	ol-sp-pig-aug rim-pl-gl
15	1270	1.4	1050	242.9	0.91	ol-sp-pig-aug rim-pl-si-gl
13	1270	1.4	1100	189.7	0.90	ol-sp-pig-aug rim-gl
14	1270	1.4	1188	93.3	0.88	ol-sp-pig-gl
22	1273	2.6	1008	98.4	2.69	ol-sp-pig-aug rim-gl
21	1272	2.6	1095	66.8	2.65	ol-sp-pig-aug rim-gl
39	1288	1.2	1149	51.9	2.68	ol-sp-pig-gl
40	1288	1.2	1204	31.6	2.66	ol-sp-gl
37	1288	2.5	959	36.5	9.03	ol-sp-pig-aug rim-gl
28	1288	8.7	1064	33.5	6.68	ol-sp-pig-aug rim-gl
30	1288	1.5	1123	20.1	8.24	ol-sp-pig-aug rim-gl
29	1288	1.5	1175	12.8	8.81	ol-sp-pig-gl
38	1288	2.5	1187	12.0	8.43	ol-sp-pig-gl
36	1270	1.7	920	3.7	94.6	ol-sp-aug-gl

[+] Experiments were held at an initial temperature for the indicated time (hours), then cooled at the specified rate and quenched into water at T fin. Temperatures given in °C.

[*] Abbreviations: ol=olivine, sp=spinel, pig=pigeonite, aug rim=augite rim, pl=plagioclase, si=silica, gl=quenched liquid. The phases indicated were in contact with the liquid, except for the pigeonite phase when mantled by augite.

Table 3. Bulk compositions of synthetic komatiites used for experiments and electron microprobe analyses of run products from 1-atmosphere experiments. See Table 1 for run conditions and abbreviations.

			Na_2O	MgO	Al_2O_3	SiO_2	K_2O	CaO	TiO_2	Cr_2O_3	MnO	FeO
comp. A, bulk			0.81	12.6	11.6	49.2	0.13	11.4	0.43	0.47	0.36	12.9
comp. B, bulk			0.37	17.2	10.6	50.1	0.07	9.5	0.33	0.41	0.36	11.0
Run #	phase	# of analyses										
Composition A												
#3	gl	4	0.53 (3)*	7.92 (11)	13.0 (2)	50.6 (6)	0.10 (2)	12.2 (3)	0.41 (2)	0.06 (5)	0.31 (6)	14.2 (2)
	ol	2		39.2 (4)	0.22 (2)	38.4 (3)		0.48 (1)		0.15 (1)	0.46 (4)	21.9 (1)
	aug	6	0.02 (1)	18.4 (4)	2.54 (25)	52.1 (4)		16.1 (7)	0.03 (2)	0.84 (9)	0.31 (3)	9.01 (38)
	pl	3	0.71 (3)	0.46 (10)	33.6 (6)	45.5 (3)	0.06 (1)	18.6 (3)				1.16 (27)
#5	gl	5	0.45 (5)	8.43 (8)	12.7 (1)	51.1 (5)	0.14 (2)	12.6 (1)	0.38 (2)	0.06 (2)	0.35 (3)	13.5 (1)
	ol	4		39.4 (6)	0.50 (46)	38.2 (8)		0.45 (1)	0.08 (1)	0.58 (43)	0.40 (2)	20.4 (2)
#1	gl	5	0.42 (5)	9.09 (17)	12.8 (1)	50.4 (1)	0.07 (1)	12.0 (1)	0.33 (2)	0.10 (2)	0.31 (4)	14.2 (1)
	ol	2		41.7 (1)	0.12 (1)	39.3 (3)		0.42 (6)		0.20 (8)	0.37 (4)	19.6 (2)
#2	gl	4	0.45 (5)	9.90 (8)	12.5 (1)	49.7 (2)	0.08 (1)	11.7 (1)	0.35 (2)	0.08 (2)	0.31 (6)	14.4 (2)
#4	gl	5	0.53 (3)	10.8 (1)	12.2 (1)	49.7 (2)	0.05 (1)	11.4 (1)	0.33 (2)	0.08 (6)	0.30 (3)	14.5 (1)
	ol			43.2 (2)	0.10 (2)	39.7 (1)		0.38 (1)		0.17 (1)	0.34 (3)	17.7 (1)
Composition B												
#4	gl	6	0.57 (5)	7.72 (5)	12.7 (1)	50.1 (2)	0.22 (2)	12.4 (3)	1.02 (24)	0.05 (3)	0.37 (2)	13.4 (2)
	ol	3		40.1 (2)	0.10 (5)	38.6 (3)		0.43 (2)		0.09 (2)	0.44 (3)	20.7 (3)
	pig	6		25.6 (3)	1.46 (11)	54.0 (4)		5.31 (33)	0.36 (30)	0.50 (7)	0.49 (14)	12.5 (2)
	pl	4	0.63 (7)	0.63 (12)	33.4 (3)	45.4 (3)	0.07 (2)	18.1 (2)				1.16 (13)
#2	gl	4	0.29 (5)	8.62 (6)	13.6 (1)	51.2 (7)	0.11 (2)	13.0 (1)	0.55 (7)	0.14 (3)	0.43 (21)	12.2 (1)
	ol	3		42.3 (9)	0.37 (26)	39.5 (7)		0.53 (28)		0.26 (23)	0.47 (2)	17.7 (1)
	pig	6		28.0 (7)	1.74 (30)	55.3 (3)		4.25 (20)		0.51 (7)	0.41 (5)	11.1 (2)
#3	gl	6	0.30 (4)	9.38 (18)	13.9 (1)	51.9 (6)	0.10 (2)	12.7 (2)	0.33 (7)	0.14 (1)	0.37 (6)	12.0 (1)
	ol	2		44.1 (7)	0.12 (5)	39.6 (2)		0.33 (1)		0.34 (29)	0.40 (1)	15.9 (6)
	pig	5		31.3 (3)	2.16 (53)	55.4 (6)		2.26 (13)		0.67 (4)	0.36 (1)	9.90 (30)
#1	gl	5	0.28 (5)	9.68 (7)	13.8 (1)	51.9 (6)	0.10 (2)	12.2 (2)	0.31 (3)	0.12 (3)	0.33 (5)	10.9 (2)
	ol	3		45.4 (4)	0.10 (3)	40.3 (3)		0.33 (4)		0.12 (5)	0.40 (3)	15.3 (3)
	pig	5		30.6 (3)	1.85 (26)	55.6 (5)		2.11 (12)		0.78 (16)	0.33 (4)	9.58 (12)
#5	gl	4	0.27 (5)	10.5 (1)	12.6 (1)	51.7 (7)	0.08 (1)	11.5 (1)	0.29 (3)	0.13 (3)	0.34 (8)	13.2 (1)
	ol	1		43.3	0.08	39.8		0.33		0.16	0.37	16.9
#6	gl	4	0.31 (6)	10.6 (2)	12.8 (1)	52.4 (7)	0.09 (1)	11.5 (1)	0.28 (2)	0.14 (5)	0.33 (4)	11.3 (3)
	ol	3		44.3 (5)	0.15 (9)	39.6 (6)		0.31 (2)		0.26 (10)	0.38 (2)	14.6 (3)
#7	gl	4	0.27 (8)	11.7 (1)	12.2 (3)	51.5 (5)	0.08 (1)	10.9 (1)	0.26 (2)	0.14 (2)	0.36 (7)	12.4 (2)
	ol	3		44.3 (7)	0.15 (1)	39.6 (4)		0.31 (1)		0.26 (25)	0.30 (5)	14.8 (1)

* Parenthesized units represent one standard deviation of replicate analyses in terms of least unit cited. Thus 0.53 (3) should be read 0.53±0.03.

reaches the olivine–augite cotectic, and follows this cotectic to the reaction point, where plagioclase and pigeonite appear. Crystallization continues with the projected position of the liquid remaining at the reaction point, while olivine + liquid react to form pigeonite, augite and plagioclase. For both compositions, the solid residue formed by equilibrium crystallization at 1-atmosphere consists of the assemblage olivine–augite–pigeonite–plagioclase±spinel. It should be noted that the liquids discussed using these simple projection schemes are chemically complex, and though their projected compositions remain at the ol–aug–pig–pl reaction point during crystallization, the FeO/MgO, TiO_2 and alkali abundances in the liquids are changing as the reaction progresses. These important minor element variations are suppressed by the projection scheme, but the mineral-component projection scheme is useful in predicting liquid line of descent and phase appearances.

Bulk composition of the komatiite flow and significance of the pyroxene spinifex zone

From the preceding discussion it is clear that the crystallization sequence obtained by experiment depends critically on the chosen starting composition, and that pigeonite, the important early crystallizing phase in the pyroxene-spinifex zone is the first low-pressure pyroxene

SYNTHETIC KOMATIITE COMPOSITIONS

A

B

that gave rise to Fred's Flow and the Alexo Flow (Arndt et al., 1977, Arndt and Fleet, 1979) are within the projected range of compositions that would precipitate pigeonite as the initial pyroxene phase (between the two dashed lines in Fig. 4) which requires the CaO/Al_2O_3 (wt.% ratio) to be less than unity. A potential problem with analyzed komatiite lavas is that they may have experienced hydrothermal alteration on the sea floor, or later metamorphic processes, which may have altered the rock compositions. As an example, Mottl and Holland (1978) find that SiO_2, Ca, K, Ba are leached from basalts during alteration by seawater. Arndt (1983) suggests that some olivine cumulates have lost CaO through alteration of their interstitial glass, and might have CaO/Al_2O_3 lower than that of the parent komatiite. Our composition B might have a low CaO/Al_2O_3 since it was calculated using the olivine cumulate layer. However, the presence of pigeonite in Fred's Flow and the Alexo flow limits the bulk composition to CaO/Al_2O_3 ratios of 0.8 or 0.9. Although the CaO/Al_2O_3 of the olivine cumulates may be low, the CaO/Al_2O_3 of the olivine and pyroxene spinifex zones is high, and the bulk composition of the parent melt for Fred's Flow and the Alexo Flow probably lies in between.

If a composition is chosen for experiments that is not representative of the liquid or some part of the liquid line of descent, the crystallization sequence inferred from it will not be consistent with the observed mineral paragenesis in the lava flow. This potential problem was noted by Arndt (1976) who chose a portion of the pyroxene spinifex-textured region for experimental study. The projected compositions of samples from this zone (Fig. 4) indicate

Fig. 2. (A) Results of synthesis experiments on two synthetic komatiite compositions. Experiments were carried out at the quartz–fayalite–magnetite (QFM) buffer. (B) Results of cooling rate experiments on synthetic komatiite composition B are tabulated on this temperature–cooling rate plot. The experiments were initiated at 1275±10°C, within the olivine + spinel stability field, cooled at a desired rate to the temperature indicated by the black dot, and quenched into water. Experiments quenched below the lines labelled pig in, aug in and plag in contain the phases in question.

Fig. 3. One-atmosphere liquidus relations for synthetic komatiite compositions. Liquids plotted in this diagram are pyroxene saturated and the lowest temperature liquids for each composition are plagioclase saturated. A and B in the olivine primary phase volume mark the bulk compositions used for the experiments. The positions of the orthopyroxene reaction curves are inferred from the experiments of Kushiro (1972) on Fo–Di–Qtz, and Grove et al. (1983) on tholeiitic and calc-alkaline systems. See Grove et al. (1982, 1983) for projection scheme.

to crystallize from some Munro township komatiite bulk compositions. An initial conclusion is that small changes in bulk composition of the parent komatiite magma can determine the presence or absence of a pigeonite-spinifex zone. If the komatiite has a relatively high ol+cpx component (or high CaO/Al_2O_3) and a low qtz value, the first pyroxene will be augite, not pigeonite. We propose that the bulk compositions of the komatiite parent liquids

Fig. 4. Bulk compositions of samples from Fred's Flow from Arndt et al. (1977) plotted in the Ol–Cpx–Qtz pseudoternary. Also shown are the 1-atmosphere cotectics and the projected compositions of the augite and pigeonite that crystallize on the 1-atmosphere cotectics and reaction curves. B is a possible bulk composition for Fred's Flow and the dotted line is a fractional crystallization path followed by this liquid. The dashed lines radiating from ol to the pigeonite reaction boundary limit the permissible part of projected composition space for komatiite flows that crystallize pigeonite.

that most would not reproduce the crystallization sequence followed by our proposed bulk composition of Fred's Flow, and that none of the samples lie on the proposed liquid line of descent. Most of the pyroxene spinifex samples lie in the olivine primary phase volume, and would crystallize augite as the initial pyroxene. In other words, these pyroxene spinifex zones do not represent chilled liquids. The suggestion that the pyroxene spinifex zones form by metastable crystallization and that these zones are representative of ultramafic liquid compositions (Arndt, 1976; Campbell and Arndt, 1982) requires reevaluation. We propose that the pyroxene spinifex zones are the residual products of fractional crystallization at the upper surface of the cooling komatiite flow, and that these zones have expelled variable amounts of their interstitial melt. The pyroxene spinifex zones could have formed when olivine fractionation moved the liquid composition into the pigeonite primary phase volume. Pigeonite nucleated at the upper solidified boundary of the flow and the pyroxene spinifex zones grew as stalactite-like projections into the interior of the flow (Barnes et al., 1983). These zones would then be mixtures of clinopyroxene "stalactites" plus some liquid. This mixture would not provide a sample of the liquid line of descent followed during fractionation.

In the following discussions we propose a fractional crystallization scheme that can account for the observed bulk compositions of the layers and for the observed mineral associations present in Fred's Flow and the Alexo Flow. Two important associations need to be reconciled with the experimental result that pigeonite is

the first stable pyroxene for both Fred's and Alexo's flows: (1) the more rapidly cooled olivine spinifex zone contains augite as the only pyroxene and (2) the cumulus layers contain the association orthopyroxene-augite. To rationalize these pyroxene associations, we must consider the effects of variable cooling rate on crystallization and the effects of magmatic processes that operated during differentiation and cooling of the flow.

Fractional crystallization of the komatiite flow

The predicted fractional crystallization path for composition B would be olivine crystallization, followed by spinel which would move residual liquid compositions away on an olivine subtraction line toward the olivine-pigeonite reaction boundary (Fig. 4). When the reaction boundary is reached, olivine is removed from contact with liquid, and the liquid moves into the pigeonite phase volume on a trajectory away from the composition of the pigeonite that is crystallizing until the pigeonite–augite cotectic is reached. Plagioclase appears as a crystallizing phase and 3-phase crystallization moves the liquid along the augite–pigeonite–plagioclase cotectic until all liquid is exhausted. Comparison of the bulk compositions of the layers in Fred's Flow with this predicted fractionation scheme (Fig. 4) indicates that to a large extent liquid and crystals interacted during the differentiation of the flow, and that highly evolved products of fractionation are not preserved in the flow. Most samples plot within the 4-phase volume (Ol–Aug–Pig–Plag), which would be expected for residues of equilibrium crystallization. Three gabbros are quartz-normative which qualifies them as mixtures of residual liquid, cumulus plagioclase, and high- and low-Ca pyroxenes. The peridotites, as expected, are olivine cumulates, and their compositions plot closest to a tie line between olivine and the composition B. The compositions of the olivine spinifex layers lie toward the augite side of the projection, and assuming that these compositions have not been modified by alteration, this may indicate that these rocks are not simple liquid + olivine cumulates. The olivine spinifex layers contain olivine, spinel, an aluminous augite and glass, (Arndt et al., 1977) and have apparently accumulated augite as well as olivine during cooling and solidification. The pyroxene spinifex layers may be cumulates of low-Ca pyroxene, augite, and plagioclase (±olivine) (Fig. 4). If the pyroxene-spinifex zones were trapped liquids they should be quartz-normative, but most samples plot close to the Aug–Pig–Plag plane in Figure 4, suggesting that the zones expelled residual melt during growth.

Effects of dynamic crystallization on differentiation

Rate experiments. The effects of variable cooling rate on phase appearance sequence and temperature are summarized in Figure 2b. All experiments were initiated in the olivine phase volume, and also contained spinel. The

curves were constructed by observing phase assemblages present in experiments cooled to a desired temperature at the indicated rate and then quenched. Experiments terminated below each line contain the phase(s) noted. The effect of increased cooling rate in suppressing phase appearance temperature is dramatic and the pyroxene relations bear a striking resemblance to those observed in other basaltic lavas that crystallize pigeonite after olivine (Walker et al., 1976; Grove and Bence, 1977, 1979; Schiffman and Lofgren, 1982; Baker and Grove, 1985). At slow cooling rates (0.5 to 3°C/hr) pigeonite appearance is not affected significantly and it crystallizes near its equilibrium appearance temperature. At faster cooling rates (>10°C/hr), pigeonite appearance is suppressed. Augite appearance temperature decreases with increasing rates and is suppressed by 50°C at 10°C/hr and by ~150°C at 100°C/hr. Plagioclase nucleation and growth is supercooled by 75°C below its equilibrium appearance temperature at 0.5°C/hr, the slowest cooling rate investigated, and does not appear as a crystallizing phase in runs cooled at 3°C/hr or greater.

Chilled margin and olivine spinifex zones. The textural association observed in the olivine spinifex zone of Fred's Flow (Fig. 1), near the upper flow margin, consists of skeletal olivine crystals in a matrix of augite, glass and spinel (Arndt et al., 1977). The spinifex olivine phenocrysts form because the olivine removed from the upper portion of the flow, either by crystal settling or by convection, leaves the liquid devoid of crystal nucleii and supercooled with respect to olivine appearance. Olivine nucleates and grows as skeletal crystals under such conditions and Donaldson (1977) provides graphic experimental verification of the supercooled effects that result as a consequence of the absence of crystal nucleii. The groundmass assemblage of augite and spinel is identical to that produced in the 100°C/hr cooling rate experiments. As shown in many kinetic experiments on basaltic compositions (Walker et al., 1976; Grove and Bence, 1979; Schiffman and Lofgren, 1982; Baker and Grove, 1985) pigeonite nucleation is inhibited during crystallization at rapid rates. Under such crystallization conditions the residual liquid passes through the pigeonite field, moves into the augite primary phase volume, becomes supersaturated with augite and precipitates an aluminous augite. Augites produced in the rapid cooling rate experiments (100°C/hour) are similar to those observed in the olivine spinifex zone of Fred's Flow (Arndt et al., 1977, Table 3). The natural and experimentally-produced augites are plotted on pyroxene quadrilaterals in Figure 5. Both the natural and experimental augites contain comparable concentrations of major and minor elements (compare Table 4 and Arndt et al., 1977, Table 3). The compositional similarity is further evidence that the augites in the olivine spinifex zone are not equilibrium phases, but are produced under conditions of rapid cooling (~100°C/hr) experienced at the upper chilled margin of Fred's Flow.

Pyroxene-spinifex textures. The textural and mineral-ogical associations found in the pyroxene-spinifex zone of the Munro Township komatiites are strikingly similar to those found in Apollo 15 quartz-normative basalts (Bence and Papike, 1972; Lofgren et al., 1974; Grove and Bence, 1977). Skeletal clinopyroxene phenocrysts contain pigeonite cores that are mantled by augite rims and surrounded by a groundmass of augite, plagioclase and oxide. In both examples the complex skeletal growth form of the pigeonite phenocryst core produces hollow internal zones that are rimmed by augite overgrowths internally and externally. In the komatiite flows the pyroxene-spinifex zone formed in the upper part of the lava flow as a consequence of cooling and differentiation. As the flow crystallized, olivine moved by settling or by convective processes from the upper portions to form the thick basal peridotitic cumulates, depleting the residual liquid in olivine in the upper portion of the flow. As olivine fractionation continued, the residual liquid composition in the upper part of the flow entered the pigeonite primary phase volume, nucleated skeletal pigeonite at a small undercooling, and initiated the growth of pyroxene-spinifex zone. This crystallization process is discussed in some detail by Grove and Raudsepp (1978) for lunar analogs. Continued pigeonite crystallization was accompanied by suppression of plagioclase appearance, driving the liquid into the augite primary phase volume at larger undercoolings. Augite then nucleated epitaxially on the pigeonite phenocrysts. Augite crystallization continued and increased the supersaturation of the residual liquid in plagioclase component. Finally, plagioclase and augite nucleated as groundmass phases. This nucleation and growth response is followed in the komatiite experiments, at cooling rates of 1.0 and 0.5°C/hr.

The pyroxene zoning trends (Fig. 5b, Table 4) from the cooling rate experiments are comparable to those found in the spinifex zones of Fred's Flow and the Alexo Flow (Arndt, 1977, Arndt and Fleet, 1979, Fig. 5a). Unfortunately, the pigeonite cores of Fred's and the Alexo Flow have been altered to chlorite, so the entire trend is not preserved in the natural samples. The most magnesian pigeonite preserved in Fred's Flow is Wo_7En_{77}. Our experiments suggest that the initial pigeonite was Wo_4En_{82}, that it formed at approximately 1200°C and that it crystallized from a liquid containing ~12 wt.% MgO (Table 3). These zoning trends record the initial near-equilibrium crystallization of pigeonite at a small value of undercooling. Continued dynamic crystallization departed from equilibrium, as recorded by the pigeonite zoning trends. Pigeonite becomes Ca and Fe enriched, and drives the residual liquid composition into the augite phase volume. As a consequence of the suppression of plagioclase nucleation, an aluminous augite grows causing supersaturation with plagioclase and resulting in the nucleation of groundmass augite + plagioclase.

Though the zoning trends in the dynamic experiments approximate closely those found in the natural samples, we were unable to reproduce the morphologies of the
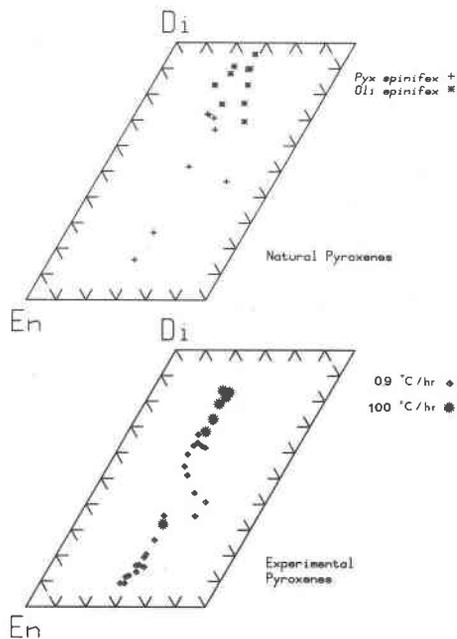
Fig. 5. (A) Pyroxene analyses from Fred's Flow and the Alexo Flow. Stars are clinopyroxene analyses from the olivine-spinifex-textured layer of Fred's Flow (Arndt et al., 1977, Table 3). Crosses are analyses from the pyroxene-spinifex layer of Fred's Flow and the Alexo Flow (Arndt, 1977; Arndt and Fleet, 1979). (B) Experimentally produced pyroxene zoning trend for 1°C/hr experiments (diamonds) and from 100°C/hr experiments (stars). Table 4 contains selected representative analyses from these trends. The 1°C/hr trend is compiled from microprobe traverses on pigeonite cores and augite rims from cooling rate experiments 13, 14 and 15 (Table 2). The 100°C/hr pyroxenes are from run 36.

pigeonite spinifex zones. The spinifex needles in Fred's Flow are up to 5 cm in length, and our experimental beads are only 0.5 cm in diameter. The experimentally produced crystals are stubby, but internally skeletal and contain pigeonite cores and augite mantles. The fine-grained groundmass produced in our experiments is also generally similar to that found in the komatiites. Another difference in our experimental charges is that the olivines are small, abundant, equant grains. We did not attempt to produce experimentally the olivine supercooling that was induced during the crystallization of the komatiite flows. Since olivine is being removed by gravitative settling or convective stirring as it forms in the komatiite flow, the residual liquids are devoid of olivine nucleii and supercooled with respect to olivine precipitation. Donaldson (1977, 1982) demonstrated that this effect can lead to the distinctive spinifex characteristic of the flow tops. Donaldson (1977, 1982) showed that the experimental cooling rates required to produce the observed textural effects were comparable to the cooling rates calculated assuming heat loss through conductive cooling near the boundary

of the flow. In the following discussion we show that the experimental cooling rates required to produce the pyroxene compositions found in the olivine- and pyroxene-spinifex layers are also reasonably close to theoretical estimates of the cooling rates predicted for these layers.

Bronzite cumulate and gabbroic zones

An interior gabbroic layer in Fred's Flow (Fig. 1) contains augite, plagioclase and orthopyroxene. There is no gabbroic unit in the Alexo Flow, but sandwiched between the pyroxene-spinifex zone and the basal olivine cumulate peridotite is a bronzite cumulate that contains olivine, orthopyroxene and chromite set in a fine-grained groundmass. For the bulk composition (Fig. 4) of the komatiite magma there is no crystallization path along which liquids can evolve to an orthopyroxene saturation surface, assuming that our inferred phase diagram topology is correct. Assume further that the orthopyroxene is not a result of later subsolidus reaction on cooling, and formed as a consequence of a closed system crystallization process, related to the late stages of differentiation of the lava flow. Mixing between residual liquids excluded from the upper portions of the lava flow by crystallization of the pyroxene spinifex-textured zone and liquids derived by olivine crystallization in the basal peridotite could stabilize orthopyroxene. In the next section we propose a magma mixing process that could have produced orthopyroxene saturation during late stage differentiation.

Cooling rates of Fred's Flow

The upper portion of Fred's Flow consists of a flowtop breccia, 6 meters thick, a 1 meter layer of olivine spinifex textured lava and an underlying 6 meter-thick pyroxene spinifex zone. Based on experimentally determined pyroxene associations the olivine spinifex zone should record cooling rates faster than 10°C/hr and the pyroxene spinifex zone should form at rates slower than 10°C/hr (Fig. 1). The gabbroic interior must form at cooling rates slower than our slowest experiment (0.5°C/hr). If the flowtop breccia is ignored, and the upper flow boundary

Table 4. Electron microprobe analyses of pyroxenes produced in cooling rate experiments. See Table 2 for run conditions.

Sample	Na₂O	MgO	Al₂O₃	SiO₂	CaO	TiO₂	Cr₂O₃	MnO	FeO
Run #15									
Core	0.04	29.67	1.29	55.59	2.38	0.00	0.65	0.41	9.22
Interior	0.00	28.80	1.72	54.55	4.21	0.00	0.67	0.44	9.50
Interior	0.00	24.95	2.63	53.67	9.00	0.03	0.91	0.38	9.39
Rim	0.02	20.5	4.39	51.98	12.94	0.09	1.10	0.37	7.93
Run #36									
Rim	0.02	15.50	6.99	50.21	19.59	0.44	0.35	0.32	7.28
Core	0.01	18.63	5.33	51.18	16.58	0.26	1.15	0.40	8.24

is chosen as the top of the olivine spinifex zone, the cooling rate estimates from textures are comparable to those predicted by theory. In a cooling submarine lava flow, heat loss through the upper boundary occurs rapidly and a constant temperature boundary condition is appropriate, while cooling from the base is slower because heat loss is by conduction. Jaeger (1968, equation 36) provides an analytical solution for the cooling of a lava flow with an upper-surface constant temperature boundary condition. Assuming a liquidus at 1400°C, solidus at 1100°C and latent heat = 80 cal/gm, the cooling rate predicted at 1 meter from the boundary is 2 to 3°C/hr, and at 6 meters the predicted rate is 0.07°C/hr. These estimates for the transition from olivine- to pigeonite-spinifex are somewhat slower, but are in reasonable accord with our experimental results. The Jaeger calculation does not include convection effects, which would speed up cooling rates in the flow and bring the experimental cooling rate estimates closer to the calculated rates.

Crystallization history of pyroxene-spinifex komatiite flows

In a thick, komatiitic lava flow differentiation by olivine removal was an important mechanism. Differentiation could have been accomplished by rapid settling of olivine crystals from the upper portion of the flow (Walker et al., 1977) or by convective processes. A proposed liquid line of descent for crystallization of the komatiite parent (path 1 in Fig. 6) begins with olivine removal, driving the residual liquid composition directly away from olivine, toward the olivine–pigeonite reaction curve. In the upper chilled margin of the flow the composition of lava samples

should lie on an olivine subtraction trend, becoming progressively depleted in olivine as one samples the flow away from the upper boundary. At some distance from the chilled margin cooling rate is slow enough that pigeonite nucleates when the residual liquid evolves to the pigeonite primary phase volume creating the pigeonite cores of the spinifex pyroxene phenocrysts (path 2 in Fig. 6). Continued cooling drives the residual liquid over the augite + plagioclase saturation boundary, and augite grows on the rims of the pigeonite phenocrysts, moving the residual liquid away from the cpx corner toward silica rich compositions (path 3 in Fig. 6). Plagioclase nucleates and the crystallization of augite and plagioclase completes the formation of the upper spinifex zone. As we suggested earlier, the pyroxene spinifex zone is not a trapped sample of a portion of the flow that was once completely liquid, but is more likely to be a collection of residual crystals plus trapped liquid. The zone is a record of the crystallization front that advanced toward the interior of the flow. First pigeonite cores grew as centimeter-long needles into the flow interior and then augite rims formed on the pigeonite cores. Finally, a groundmass of augite and plagioclase precipitated. This crystallization process generated a solidification front that advanced into the flow interior, probably trapped some interstitial melt in the network of pyroxene-spinifex needles, but also expelled some residual liquid. Hence, some fractionation occured during the development of this zone, and some residual liquid was concentrated in the central interior portion of the flow.

Figures 7a and 7b show calculated densities for the proposed liquid line of descent plotted in Figure 6. Olivine crystallization removes dense network-modifying components from the melt, leaves the lighter network-forming units in the residual liquid and causes the density of the residual liquid to decrease. Pyroxene crystallization removes dense network modifiers and light network formers in nearly equal proportions, and pigeonite and augite crystallization causes a slight density decrease. When plagioclase and augite crystallize, residual liquid density increases dramatically since plagioclase removes the light network-forming components from the melt, concentrating the dense network modifiers. The density-differentiation relations depicted in Figure 7b are similar to those found in other basaltic systems (Stolper and Walker, 1980; Grove and Baker, 1983) and show a density minimum and an associated upturn as crystallization advances.

Because heat loss in the lava flow is faster at the upper boundary and slower at the base (Jaeger, 1968), crystallization at the top and bottom of the komatiite flow proceeds at different rates. If the density relations are considered along with the crystallization history of the flow, the initial effect of olivine differentiation and cooling which occurs primarily from the top of the flow, will be to form a stable density stratified melt with hot dense less-differentiated liquid at the base of the flow and lighter

Fig. 6. Schematic crystallization history for pigeonite-bearing Munro township komatiite flow. Open star is a possible bulk composition of the komatiite parent melt. Solid lines are the experimentally determined cotectics. Dashed line is a fractionation path discussed in the text, and numbers refer to the steps in the fractionation process. The double line points to compositions of liquids, one olivine-normative and one that is a highly evolved product of fractionation that mix in the komatiite flow interior to produce bulk compositions (solid star) that will crystallize orthopyroxene.

Fig. 7. (A) Calculated fractionation path that was illustrated in Fig. 6. Star represents an assumed bulk composition for Fred's Flow in equilibrium with Fo_{94} olivine. A fractionation calculation removed olivine, then pigeonite, and finally augite and plagioclase that were calculated to be in equilibrium with the residual liquid composition at each fractionation step. The residual liquid compositions were used to calculate melt densities that are plotted in B against the normalized $ol/(ol+qtz)$ component of the pseudoternary. Density calculation procedure is the same as that described in Grove and Baker (1983).

cooler evolved liquid near the upper chilled margin. These density relations will persist in the upper part of the flow through the crystallization of olivine, the pigeonite cores and the augite rims of the pyroxene-spinifex zones, but the growth of groundmass augite + plagioclase causes a rapid increase in the density of the residual liquid. This residual liquid, which is concentrated into the flow interior as the spinifex zone forms, is denser and cooler than the underlying olivine-saturated liquid in the basal portion of the flow interior. Thus, it may mix with the underlying olivine normative liquid that has been concentrated above the basal, cumulate peridotite (path 4, Fig. 6) and the resulting mixed magma subsequently crystallizes to form the bronzite cumulate and/or gabbroic interior (path 5, Fig. 6). The composition of the mixed liquid lies in the olivine primary phase volume and this liquid precipitates olivine and reaches the orthopyroxene primary phase volume upon crystallization. Thus, mixing of evolved liquids in the flow interior can explain the occurrence of bronzite as a crystallizing phase in the interior portions of Fred's Flow and the Alexo Flow. This proposed mixing process places further constraints on the bulk composition of the komatiite lava flow. In Fred's Flow, for example, the upper portion of the lava flow that has

crystallized by the time that the pyroxene-spinifex zone has formed is approximately 12% of the total flow volume. To this volume some unknown amount of cumulus olivine must be added. If we assume that this 12% is a residue of 50% fractional crystallization, then the liquid remaining in the interior and base of the flow mixed with approximately 12% evolved liquid expelled from the upper portion of the flow. Thus, the bulk composition of the mixed liquid would lie along the mixing line (Fig. 6) close to the olivine normative member of the mix. If mixing is the cause for the appearance of orthopyroxene as a crystallizing phase in the flow interior, the projected bulk composition of Fred's Flow must lie at a higher Qtz value on the Ol–Cpx–Qtz projection (Fig. 4) than that of composition B.

Based on the 1-atmosphere phase relations one would predict both pigeonite and augite to follow orthopyroxene during the crystallization of the flow interior. Augite is present, but pigeonite, which should be in reaction relation with orthopyroxene in the flow interior is absent. The absence of pigeonite may result because, (1) the 1-atmosphere phase diagram for komatiites has a pigeonite phase volume topology that differs from the one inferred in Figure 3, (2) pigeonite nucleation is kinetically suppressed and orthopyroxene continues to crystallize, moving the residual liquid into the augite phase volume and triggering augite nucleation under conditions of modest supercooling, or (3) pigeonite is not preserved in the slowly cooled flow interior, because it transforms to the equilibrium assemblage orthopyroxene + augite at subsolidus conditions. As we have seen in the case of the chilled margins of the komatiite lava and in kinetic experiments on basalts, the second mechanism, where pigeonite growth is delayed, is an important one and possibly a common kinetic phenomenon that can alter the liquid line of descent and phase appearance sequence from that predicted by equilibrium crystallization. Alternatively, some of the orthopyroxene textural associations illustrated by Arndt and Fleet (1979, their Fig. 7) may be a consequence of subsolidus reequilibration of primary pigeonite, favoring the third mechanism. Our discussion is necessarily simplistic in the sense that we are restricting consideration to a closed system process. Barnes et al. (1983) have shown that the bronzite layer in the Alexo Flow may form by open system processes by influx of new magma into the partly solidified flow. Such a dynamic model is probably more realistic for the evolution of these flows, and the effects of recharge by new magma could produce the complications that we are trying to explain by within-flow magma mixing.

To summarize, equilibrium and kinetic experiments performed on a komatiite composition have allowed the prediction of the crystallization and differentiation history of Archean komatiites from Ontario. Kinetic factors have exercised important influences on the course of differentiation. The chill margins of the komatiite lavas contain skeletal olivine crystals in a groundmass of Al-rich augite,

spinel and glass. This assemblage is formed as a consequence of rapid cooling under disequilibrium conditions. Interior to this olivine spinifex layer, slower cooling and efficient differentiation by olivine removal generated a quartz-normative liquid that precipitated pigeonite under slightly supercooled conditions. Following pigeonite nucleation, the residual liquid departed from equilibrium, crystallizing augite at a higher degree of supercooling and finally plagioclase and augite under conditions that departed dramatically from equilibrium. Liquids derivative from the crystallization of this upper layered sequence may have segregated to the flow interior and mixed with the olivine-normative melts derived from the base to produce liquids that crystallized orthopyroxene as cooling and solidification of the flow interior continued.

Note added in proof

In this manuscript, we restricted our discussion of the evolution of Munro township komatiite flows to closed system crystallization processes. A recent paper by Huppert et al. (1984) suggests that the thermal energy in a komatiite magma is sufficient to allow assimilation of the surface rocks over which the lava flows. Assimilation by surface thermal erosion of a small amount of silicic crustal component changes the bulk composition of the evolved lavas in a direction that stabilizes pigeonite as the first pyroxene to crystallize. Continued assimilation would stabilize orthopyroxene. For example, in Fig. 4 a proposed silicic contaminant would plot near the Qtz apex. A small amount of assimilation of this silicic crustal melt and accompanying olivine crystallization would move the Fred's Flow flowtop composition (which crystallizes augite as the first pyroxene) into a part of composition space where pigeonite is the first pyroxene to precipitate. Therefore, within the context of a magmatic system open to assimilation of a crustal component, it is possible to rationalize the complex pyroxene associations found in the Munro township komatiites.

In our study, we rejected the chilled margin composition of Fred's Flow as representative of the parent melt for komatiite flows that crystallized pigeonite. We favored a bulk composition calculated by averaging analyses of cumulates from the flow interior and correcting this average for olivine addition. Within the framework of a magma system open to assimilation, our objection to the flowtop as a parent melt composition is no longer necessary. The flowtop could be the uncontaminated parent melt, which chilled soon after eruption, experiencing no assimilation. The lavas in the flow interior interacted with the ground over which the flow channel was established and changed composition by assimilation of this surface material. The pyroxene associations are consistent with the changes in bulk composition expected to result from assimilation. The chilled margin has a lower Qtz component (Fig. 4) and has augite as its first pyroxene. The flow interiors changed composition by assimilation toward the

Qtz apex, stabilizing either pigeonite or orthopyroxene as the initial pyroxene.

References

Albee, A. L. and Ray, L. (1970) Correction factors for electron probe microanalysis of silicates, oxides, carbonates, phosphates and sulfates. Analytical Chemistry, 42, 1408–1414.

Arndt, N. T. (1976) Melting relations of ultramafic lavas (komatiites) at one-atmosphere and high pressure. Carnegie Institute of Washington Yearbook 75, 551–561.

Arndt, N. T. (1977) Mineralogical and chemical variation in two thick layered komatiitic lava flows. Carnegie Institute of Washington Yearbook, 76, 494–501.

Arndt, N. T. (1983) Element mobility during komatiite alteration. (abstr.) EOS, Transactions, American Geophysical Union, 64, 331.

Arndt, N. T. and Fleet, M. E. (1979) Stable and metastable pyroxene crystallization in layered komatiite lava flows. American Mineralogist, 64, 836–864.

Arndt, N. T., Naldrett, A. J., and Pyke, D. R. (1977) Komatiitic and iron-rich tholeiitic lavas of Munro Township, northeast Ontario. Journal of Petrology, 18, 319–369.

Baker, M. B. and Grove, T. L. (1985) Kinetic controls on pyroxene nucleation and liquid lines of descent in a basaltic andesite. American Mineralogist, 70, in press.

Barnes, Sarah-Jane, Gorton, M. P. and Naldrett, A. J. (1983) A comparative study of olivine and clinopyroxene spinifex flows from Alexo, Abitibi greenstone belt, Ontario, Canada. Contributions to Mineralogy and Petrology, 83, 293–308.

Bence, A. E. and Albee, A. L. (1968) Empirical correction factors for the microanalysis of silicates and oxides. Journal of Geology, 76, 382–403.

Bence, A. E. and Papike, J. J. (1972) Pyroxenes as recorders of lunar basalt petrogenesis: chemical trends due to crystal-liquid interaction. Proceedings of the Third Lunar Science Conference, 431–469.

Campbell, I. H. and Arndt, N. T. (1982) Pyroxene accumulation in spinifex-textured rocks. Geological Magazine, 119. 605–610.

Donaldson, C. H. (1977) Laboratory duplication of comb layering in the Rhum pluton. Mineralogical Magazine, 41, 323–336.

Donaldson, C. H. (1982) Spinifex-textured komatiites: a review of textures, compositions and layering. In N. T. Arndt and E. G. Nisbet, Eds., Komatiites, p. 213–244. George Allen and Unwin, Boston.

Grove, T. L. (1981) Use of FePt alloys to eliminate the iron loss problem in 1-atmosphere gas mixing experiments: Theoretical and practical considerations. Contributions to Mineralogy and Petrology, 78, 298–304.

Grove, T. L. and Baker, M. B. (1983) Effects of melt density on magma-mixing in calc-alkaline series lavas. Nature, 305, 416–418.

Grove, T. L. and Bence, A. E. (1977) Experimental study of pyroxene-liquid interaction in quartz-normative basalt 15597.

Proceedings of the 8th Lunar Science Conference, 1549–1579.

Grove, T. L. and Bence, A. E. (1979) Crystallization kinetics in a multiply saturated basalt magma: an experimental study of Luna 24 ferrobasalt. Proceedings of the 10th Lunar and Planetary Science Conference, 439–478.

Grove, T. L., Gerlach, D. C. and Sando, T. W. (1982) Origin of calc-alkaline series lavas at Medicine Lake volcano by fractionation, assimilation and mixing. Contributions to Mineralogy and Petrology, 80, 160–182.

Grove, T. L., Gerlach, D. C., Sando, T. W. and Baker, M. B. (1983) Origin of calc-alkaline series lavas at Medicine Lake volcano by fractionation, assimilation and mixing: corrections and clarifications. Contributions to Mineralogy and Petrology, 82, 407–408

Grove, T. L. and Raudsepp, M. (1978) Effects of kinetics on the crystallization of quartz-normative basalt 15597: An experimental study. Proceedings of the 9th Lunar and Planetary Science Conference, 585–599.

Huppert, H. E., Sparks, R. S. J., Turner, J. S. and Arndt, N. T. (1984) Emplacement and cooling of komatiite lava flows. Nature, 309, 19–22.

Jaeger, J. C. (1968) Cooling and solidification of igneous rocks. In H. H. Hess and A. Poldevaart, Eds., Basalts, the Poldevaart Treatise on Rocks of Basaltic Composition, p. 503–536. Wiley, New York.

Kushiro, I. (1972) Determination of the liquidus relations in synthetic silicate systems with electron probe analysis: the system forsterite–diopside–silica at 1 atmosphere. American Mineralogist, 57, 1260–1271.

Lofgren, G., Donaldson, C. H., Williams, R. J., Mullins, O., Jr. and Usselman, T. M. (1974) Experimentally reproduced textures and mineral chemistry of Apollo 15 quartz-normative basalts. Proceedings of the Fifth Lunar Science Conference, 549–567.

Mottl, M. J. and Holland, H. D. (1978) Chemical exchange during hydrothermal alteration by seawater—I. Experimental results for major and minor components of seawater. Geochimica et Cosmochimica Acta, 42, 1103–1116.

Schiffman, Peter and Lofgren, G. E. (1982) Dynamic crystallization studies on the Grande Ronde pillow basalts, central Washington. Journal of Geology, 90, 49–78.

Stolper, Edward and Walker, David (1980) Melt density and the average composition of basalt. Contributions to Mineralogy and Petrology, 74, 7–12.

Walker, David, Shibata, T. and DeLong, S. F. (1979) Abyssal tholeiites from the Oceanographer Fracture Zone II, Phase equilibrium and mixing. Contributions to Mineralogy and Petrology, 70, 111–125.

Walker, David, Kirkpatrick, R. J. and Harp, J. F. (1977) Differentiation of a komatiite lava. (abstr.) EOS, Transactions, American Geophysical Union, 58, 527.

Walker, David, Kirkpatrick, R. J., Longhi, J. and Hays, J. F., (1976) Crystallization history of lunar picritic basalt sample 12002: Phase equilibria and cooling rate studies. Geological Society of America Bulletin, 87, 646–656.